

Observational constraints on interacting dark matter model without dark energy

Shuo Cao, Zong-Hong Zhu and Nan Liang

Department of Astronomy, Beijing Normal University, Beijing 100875, China
e-mail: zhuzh@bnu.edu.cn, liangn@bnu.edu.cn

Preprint online version: November 26, 2021

ABSTRACT

Aims. The interacting dark matter (IDM) scenario allows for the acceleration of the Universe without Dark Energy.

Methods. We constrain the IDM model by using the newly revised observational data including $H(z)$ data and Union2 SNe Ia via the Markov chain Monte Carlo method.

Results. When mimicking the Λ CDM model, we obtain a more stringent upper limit to the effective annihilation term at $\kappa C_1 \approx 10^{-3.4} \text{Gyr}^{-1}$, and a tighter lower limit to the relevant mass of Dark Matter particles at $M_x \approx 10^{-8.6} \text{Gev}$. When mimicking the w CDM model, we find that the effective equation of state of IDM is consistent with the concordance Λ CDM model and appears to be most consistent with the effective phantom model with a constant EoS for which $w < -1$.

Key words. Cosmology: dark matter — cosmological observations

1. Introduction

Recent observations of type Ia supernovae (SNe Ia, Riess et al. 1998; Perlmutter et al. 1999) have predicted that our present universe is passing through an accelerated phase of expansion preceded by a period of deceleration. A new type of matter with negative pressure, which is popularly known as dark energy, has been proposed to explain the present phase of acceleration. The most simple dark energy candidate, the cosmological constant (Λ CDM model), though known to be consistent with various observations such as SNe Ia, the galaxy cluster gas mass fraction data (Wilson et al. 2006; Davis et al. 2007; Allen et al. 2008), and the CMB temperature and polarization anisotropies (Jassal et al. 2010), is always affected by the coincidence problem. Until now, many other dark energy models have been brought forward to explain this comic acceleration such as the scalar fields with a dynamical equation of state [e.g., quintessence (Peebles & Ratra 1988a, 1988b; Caldwell, Dave, & Steinhardt 1998), phantom (Caldwell 2002), k-essence (Armendariz-Picon et al. 2001), quintom (Feng et al. 2005; Guo et al. 2005; Liang et al. 2009)], the Chaplygin gas (Kamenshchik et al. 2001; Bento et al. 2002), holographic dark energy (Cohen 1999; Li 2004), and so on. Many alternatives to dark energy in which gravity is modified have been proposed as a possible explanation of the acceleration [e.g., the braneworld models (Dvali, Gabadadze, & Porrati 2000; Zhu & Alcaniz 2005), the Cardassian expansion model (Freese & Lewis 2002, Zhu & Fujimoto 2002)], as well as the $f(R)$ theory (Capozziello & Fang 2002; Carroll et al. 2004) and the $f(T)$ theory (Bengochea & Ferraro 2009; Wu & Yu 2010).

It has been shown that the dark matter self-interactions could provide the accelerated expansion of the Universe without any dark energy component (Zimdahl et al. 2001; Balakin et al. 2003). In the framework of the Boltzmann formalism, if there is a disequilibrium between the dark matter particle creation and annihilation processes, an effective source term with negative pressure could be created. Basilakos & Plionis (2009) in-

vestigated the circumstances under which the analytical solution space within the framework of the interacting dark matter (IDM) scenario allows for a late accelerated phase of the Universe, and find that the effective annihilation term of the simplest IDM model is quite small by using the nine observational $H(z)$ data points of Simon et al. (2005). The gravitational matter creation model that is fully dominated by cold dark matter (Lima et al. 2008; Basilakos & Lima 2010) is mathematically equivalent to one case of the IDM models (Basilakos & Plionis 2009).

In this paper, we use the newly revised $H(z)$ data (Stern et al. 2010; Gaztañaga et al. 2009) and the Union2 set of 557 SNe Ia (Amanullah et al. 2010) to constrain the relevant IDM models (Basilakos & Plionis 2009) by using the Markov chain Monte Carlo (MCMC) method. This paper is organized as follows. In Sect. 2, we briefly indicate the basic equations of the IDM models. Observational data including $H(z)$ and SNe Ia are given in Sect. 3. In Sect. 4, MCMC constraint results from different combined data sets are illustrated. Finally, we summarize our main conclusions in Sect. 5.

2. The basic equations of the IDM models

We assume that the IDM density obeys the collisional Boltzmann equation (Kolb & Turner 1990)

$$\dot{\rho} + 3H\rho + \kappa\rho^2 - \Psi = 0, \quad (1)$$

where Ψ is the rate of creation of DM particle pairs and the annihilation parameter $\kappa = \langle\sigma u\rangle/M_x$ (where M_x is the mass of the DM particle, σ is the cross-section for annihilation, and u is the mean particle velocity). Compared to the usual fluid equation, the effective pressure term is

$$p_{\text{eff}} = (\kappa\rho^2 - \Psi)/3H. \quad (2)$$

When the IDM particle creation term is larger than the annihilation term ($\kappa\rho^2 - \Psi > 0$), IDM may serve as a negative pressure source in the global dynamics of the Universe (Zimdahl et

al. 2001; Balakin et al. 2003). Basilakos & Plionis (2009) phenomenologically identified two functional forms for which the previous Boltzmann equation can be solved analytically, only one of which is of interest since it indicates the dependence of the scale factor on a “ $\propto a^{-3}$ ”. We refer to appendix B in Basilakos & Plionis (2009) for details. We assume that

$$\Psi(a) = aH(a)R(a) = C_1(n+3)a^n H(a) + \kappa C_1^2 a^{2n}. \quad (3)$$

And the total energy density is

$$\rho(a) = C_1 a^n + a^{-3} \frac{F(a)}{\left[C_2 - \int_1^a x^{-3} f(x) F(x) dx \right]}, \quad (4)$$

where n , C_1 , and C_2 are the corresponding constants of the problem (κC_1 in the unit of Gyr^{-1}), and the kernel function $F(a) = \exp[-2\kappa C_1 \int_1^a x^{n-1}/H(x) dx]$. The first term on the right side of Eq.(4) obviously corresponds to the residual matter creation that results from the possible disequilibrium between the IDM particle creation and annihilation processes, while the second term can be viewed as the energy density of the self IDM particles that are dominated by the annihilation process.

2.1. Model 1: Mimicking the Λ CDM Model

If $n = 0$, the global density evolution can be transformed as

$$\rho(a) = C_1 + a^{-3} \frac{e^{-2\kappa C_1(t-t_0)}}{[C_2 - \kappa Z(t)]}, \quad (5)$$

where $Z(t) = \int_{t_0}^t a^{-3} e^{-2\kappa C_1(t-t_0)}$ (Basilakos & Plionis 2009). At the present epoch, the density evolves according to $\rho(a) \simeq C_1 + a^{-3}/C_2$, which is approximately equivalent to the corresponding evolution in the Λ CDM model, in which the C_1 term resembles the cosmological constant term (ρ_Λ) and the $1/C_2$ term resembles the density of matter (ρ_m). The Hubble parameter can be written as (Basilakos & Plionis 2009)

$$\left(\frac{H}{H_0} \right)^2 = \Omega_{1,0} + \Omega_{2,0} a^{-3} \frac{e^{-2\kappa C_1(t-t_0)}}{1 + \kappa C_1 (\Omega_{2,0}/\Omega_{1,0}) Z(t)}, \quad (6)$$

where $\Omega_{1,0} = 8\pi G C_1 / 3H_0^2$ and $\Omega_{2,0} = 8\pi G / 3H_0^2 C_2$, which relate to Ω_Λ and Ω_{m0} in the Λ CDM model, respectively. The mass of the DM particle can also be related to the range of κC_1 (Basilakos & Plionis 2009)

$$M_x = \frac{1.205 \times 10^{-12} \langle \sigma u \rangle}{\kappa C_1} 10^{-22} \text{ GeV}. \quad (7)$$

2.2. Model 2: Mimicking the w CDM Model

When the annihilation term is negligible ($\kappa = 0$) and the particle creation term dominates, it is straightforward to obtain the evolution of the total energy density (Basilakos & Plionis 2009)

$$\rho(a) = C_1 a^n + (1/C_2) a^{-3}. \quad (8)$$

The conditions $n > -2$ implies that the IDM fluid has an inflection point, and the current model acts as the w CDM model with a constant EoS with $w_{\text{IDM}} = -1 - n/3$, but with a totally different intrinsic nature. This situation is mathematically equivalent to the gravitational DM particle creation process within the context of non-equilibrium thermodynamics (Lima et al. 2008). The Hubble parameter is now given by

$$\left(\frac{H}{H_0} \right)^2 = \Omega_{1,0} a^n + \Omega_{2,0} a^{-3}, \quad (9)$$

where $\Omega_{2,0} = 8\pi G(C_2 - C_1)/3H_0^2$ and $\Omega_{1,0} = 8\pi G C_1/3H_0^2$, respectively (Basilakos & Plionis 2009).

3. Observational data

To constrain the relevant IDM models (Basilakos & Plionis 2009), we use the newly revised $H(z)$ data (Stern et al. 2010; Gaztañaga et al. 2009) and the Union2 set of 557 SNe Ia (Amanullah et al. 2010).

3.1. The observational $H(z)$ data

It is known that the Hubble parameter $H(z)$ depends on the differential age as a function of redshift z in the form

$$H(z) = -\frac{1}{1+z} \frac{dz}{dt}, \quad (10)$$

which provides a direct measurement on $H(z)$ based on dz/dt . Jimenez et al. (2003) demonstrated the feasibility of this method by applying it to a $z \sim 0$ sample. Moreover, compared with other observational data, it is more rewarding to investigate the observational $H(z)$ data directly, because it can take the fine structure of $H(z)$ into consideration and then use the important information that this structure provides.

By using the differential ages of passively evolving galaxies determined from the Gemini Deep Deep Survey (GDDS) (Abraham et al. 2004) and archival data (Treu et al. 2001, 2002; Nolan et al. 2003a, 2003b), Simon et al. (2005) determined nine values of the Hubble parameter $H(z)$ in the range $0 \leq z \leq 1.8$, which have been used to constrain the parameters of various dark energy models (Samushia & Ratra 2006; Wei & Zhang 2007; Wu & Yu 2007a, 2007b; Zhang & Zhu 2007; Kurek & Szydlowski 2007; Lazkoz & Majerotto 2007; Sen & Scherrer 2008; Yi & Zhang 2007; Wan et al. 2007; Xu et al. 2008; Zhai, Wan, & Zhang 2010). The $H(z)$ data at 11 different redshifts were determined from the differential ages of red-envelope galaxies (Stern et al. 2010), and two more Hubble parameter data points $H(z = 0.24) = 79.69 \pm 4.61$ and $H(z = 0.43) = 86.45 \pm 5.96$ were obtained by Gaztañaga et al. (2009) from observations of BAO peaks [for a review of the observational $H(z)$ data, see Zhang & Ma (2010)]. Studies using these newly $H(z)$ data for cosmological constraint include Gong et al. (2010), Liang et al. (2010a), Liang & Zhu (2010), Cao & Liang (2010), Ma & Zhang (2011), and Xu & Wang (2010c). We emphasize the use of the Hubble constant H_0 in our analysis. Many previous have determined its present value. Freedman et al. (2001) presented the final results of the Hubble Space Telescope (*HST*) key project that measured the Hubble constant $H_0 = 72 \pm 8 \text{ km s}^{-1} \text{ Mpc}^{-1}$, Gott et al. (2001) and Chen et al. (2003) proposed that $H_0 = 68 \text{ km s}^{-1} \text{ Mpc}^{-1}$ was a more likely value, and Tammann et al. (2008) obtained $H_0 = 62.3 \pm 1.3 \text{ km s}^{-1} \text{ Mpc}^{-1}$ from 28 independently calibrated Cepheids and the distant, Cepheid-calibrated SNe Ia. More recently, Riess et al. (2009) determined $H_0 = 74.2 \pm 3.6 \text{ km s}^{-1} \text{ Mpc}^{-1}$ by combining the observations of 240 Galactic Cepheid variables using *HST*. In this work, we follow Basilakos & Plionis (2009) and adopt $H_0 = 72 \pm 8 \text{ km s}^{-1} \text{ Mpc}^{-1}$. The observational $H(z)$ data are given in Table 1. In this case, χ^2 can be defined as

$$\chi_H^2 = \sum_i^{14} \frac{(H - H_{\text{obs}})^2}{\sigma_H^2}. \quad (11)$$

z	0	0.1	0.17	0.24	0.27	0.4	0.43	0.48	0.88	0.9	1.3	1.43	1.53	1.75
$H(z)$	72	69	83	79.69	77	95	86.45	97	90	117	168	177	140	202
1σ uncertainty	± 8	± 12	± 8	± 4.61	± 14	± 17	± 5.96	± 60	± 40	± 23	± 17	± 18	± 14	± 40

Table 1. The observational $H(z)$ data (Stern et al. 2010; Gaztañaga et al. 2009; Freedman et al. 2001)

3.2. The observational SNe Ia data

SNe Ia have long been used as ‘‘standard candles’’. It is commonly believed that measuring both their redshifts and apparent peak fluxes gives a direct measurement of their luminosity distances, thus SNe Ia provide the strongest constraints on the cosmological parameters (Riess et al. 2004, 2007; Astier et al. 2006; Davis et al. 2007; Wood-Vasey et al. 2007; Kowalski et al. 2008; Hicken et al. 2009; Chen et al. 2010). The present analysis uses the Union2 (557 sample) data set of the Supernova Cosmology project covering a redshift range $0.015 \leq z \leq 1.4$ (Amanullah et al. 2010), which was used to constrain cosmological models in Wei (2010), Liang et al. (2010a, 2010b), Liang et al. (2011), Xu & Wang (2010a, 2010b), and Wang et al. (2010).

In the calculation of the likelihood from SNe Ia, we marginalize the nuisance parameter by minimizing (Di Pietro & Claeskens 2003),

$$\chi_{\text{SNe}}^2 = A - \frac{B^2}{C} + \ln\left(\frac{C}{2\pi}\right), \quad (12)$$

where $A = \sum_i^{557} (\mu^{\text{data}} - \mu^{\text{th}})^2 / \sigma_i^2$, $B = \sum_i^{557} (\mu^{\text{data}} - \mu^{\text{th}}) / \sigma_i^2$, $C = \sum_i^{557} 1 / \sigma_i^2$, and the distance modulus is $\mu = 5 \log(d_L / \text{Mpc}) + 25$, with the 1σ uncertainty σ_i from the observations of SNe Ia and the luminosity distance d_L as a function of redshift z ,

$$d_L = (1+z) \int_0^z \frac{cdz'}{H(z')}. \quad (13)$$

4. Constraint results

We define the total likelihood to be the product of the separate likelihoods of the two cosmological probes, in other words,

$$\chi_{\text{total}}^2 = \chi_H^2 + \chi_{\text{SNe}}^2. \quad (14)$$

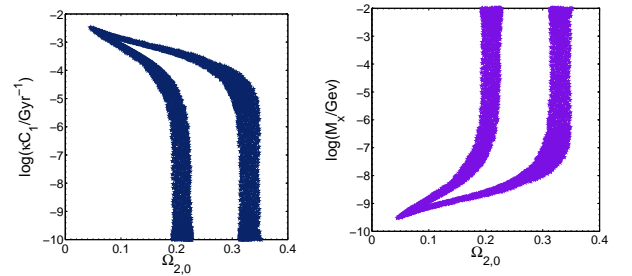
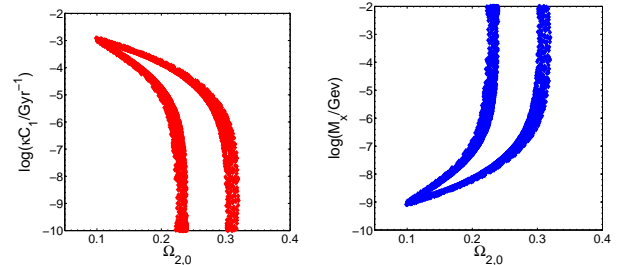
To determine the best-fit cosmological parameters, we use a χ^2 minimization and the 68.3% and 95.4% confidence levels are defined by the conventional two-parameters χ^2 levels 2.30 and 6.17, respectively. We perform a global fitting to determine the cosmological parameters using the Markov chain Monte Carlo (MCMC) method and our MCMC code is based on the publicly available package COSMOMC (Lewis & Bridle 2002).

4.1. Model 1: Mimicking the Λ CDM Model

In this model, there are two free parameters: $\Omega_{2,0}$ and κC_1 (or M_x) for a flat background ($\Omega_{1,0} + \Omega_{2,0} = 1$). In this paper, we follow Basilakos & Plionis (2009) and adopt $t_0 = 1/H_0 = 13.6$ Gyrs (roughly the age of the universe in the corresponding Λ CDM cosmology). The constraint results from different data combinations are shown in Fig. 1 - 3 and summarized in Table 2.

In Fig. 1, we show the results from the $H(z)$ data. The best-fit solution corresponds to fit $\Omega_{2,0} = 0.270^{+0.044}_{-0.044}$ and $\log(\kappa C_1 \cdot \text{Gyr}) \approx -6.85$ with an upper limit $\log(\kappa C_1 \cdot \text{Gyr}) \approx -3$. This effective annihilation term is obviously still unconstrained towards lower values. Correspondingly, the best-fit value of M_x

Model 1	$H(z)$	SNe	$H(z)$ +SNe
χ_{min}^2	9.86	544.13	554.34
$\Omega_{2,0}$	$0.270^{+0.044}_{-0.044}$	$0.271^{+0.033}_{-0.031}$	$0.272^{+0.028}_{-0.029}$
$\log(\kappa C_1 \cdot \text{Gyr})$	$-6.85(\leq -3)$	$-4.42(\leq -3.5)$	$-5.35(\leq -3.4)$
$\log M_x / \text{Gev}$	$-5.15(\geq -9)$	$-7.58(\geq -8.5)$	$-6.65(\geq -8.6)$

Table 2. Summarizing the results of parameter constraints from model 1 considered in this work. We adopt $t_0 = 1/H_0 = 13.6$ Gyrs in the computations.

Fig. 1. The likelihood contours at the 68.3% and 95.4% confidence levels in the $\Omega_{2,0} - \kappa C_1$ and $\Omega_{2,0} - M_x$ planes provided by fitting model 1 to the $H(z)$ data.

Fig. 2. The likelihood contours at the 68.3% and 95.4% confidence levels in the $\Omega_{2,0} - \kappa C_1$ and $\Omega_{2,0} - M_x$ planes provided by fitting model 1 to the SNe Ia data.

is $\log M_x / \text{Gev} \approx -5.15$ with a relatively stringent lower limit of $\log M_x / \text{Gev} \approx -9$. These results are consistent with previous work that uses fewer observational $H(z)$ data $\Omega_{2,0} = 0.3^{+0.05}_{-0.08}$ and $\log(\kappa C_1 \cdot \text{Gyr}) \approx -9.3$ (Basilakos & Plionis 2009). In Fig. 2, we show the constraint results from SNe Ia with the best-fit model parameters $\Omega_{2,0} = 0.271^{+0.033}_{-0.031}$ and $\log(\kappa C_1 \cdot \text{Gyr}) \approx -4.42$. A more stringent upper limit is obtained at around $\log(\kappa C_1 \cdot \text{Gyr}) \approx -3.5$. The best-fit DM particle mass is $\log M_x / \text{Gev} \approx -7.58$ with a relatively stringent lower limit $\log M_x / \text{Gev} \approx -8.5$. To obtain a tighter constraint on the model parameters, we combine the $H(z)$ and SNe Ia data, and the results are shown in Fig. 3. The best-fit model parameters are $\Omega_{2,0} = 0.272^{+0.028}_{-0.029}$ and $\log(\kappa C_1 \cdot \text{Gyr}) \approx -5.35$ with a much more stringent upper limit

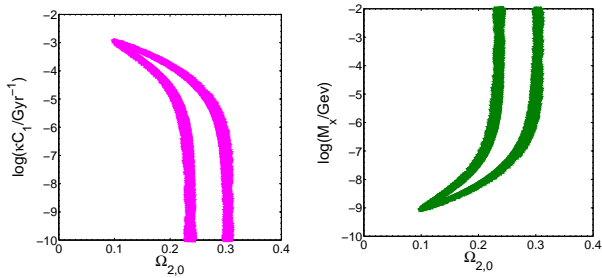


Fig. 3. The likelihood contours at the 68.3% and 95.4% confidence levels in the $\Omega_{2,0} - \kappa C_1$ and $\Omega_{2,0} - M_x$ planes provided by fitting model 1 to the $H(z)$ +SNe data.

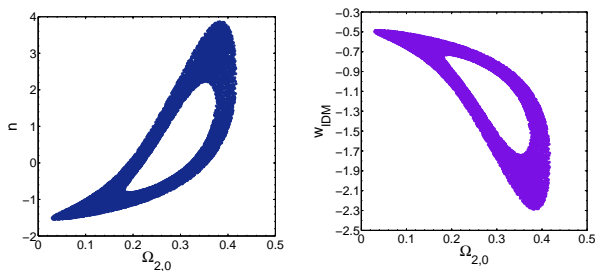


Fig. 4. The likelihood contours at the 68.3% and 95.4% confidence levels in the $\Omega_{2,0} - n$ and $\Omega_{2,0} - w_{\text{IDM}}$ planes provided by fitting model 2 to the $H(z)$ data.

$\log(\kappa C_1 \cdot \text{Gyr}) \approx -3.4$. Moreover, the best-fit value of M_x is $\log M_x/\text{GeV} \approx -6.65$ with a relatively stringent lower limit of $\log M_x/\text{GeV} \approx -8.6$ at 2σ . Since M_x is unbound at small values, it is consistent with currently accepted lower bounds of M_x (10GeV) (see Cirelli et al.(2009) and references therein).

4.2. Model 2: Mimicking the w CDM model

In this case, there are two free parameters: $\Omega_{2,0}$ and n (or w_{IDM}). The constraint results from different data combinations are shown in Fig. 4 - Fig. 6 and summarized in Table 3.

Model 2	$H(z)$	SNe	$H(z)$ +SNe
χ^2_{min}	9.40	544.12	554.39
$\Omega_{2,0}$	$0.277^{+0.098}_{-0.097}$	$0.288^{+0.108}_{-0.105}$	$0.281^{+0.072}_{-0.071}$
n	$0.70^{+1.54}_{-1.54}$	$0.17^{+1.10}_{-1.10}$	$0.22^{+0.67}_{-0.66}$
w_{IDM}	$-1.23^{+0.51}_{-0.51}$	$-1.06^{+0.37}_{-0.37}$	$-1.07^{+0.24}_{-0.23}$

Table 3. Summarizing the results of constraint on parameters from model 2.

For the $H(z)$ data and the results shown in Fig. 4, the best-fit parameter values are $\Omega_{2,0} = 0.277^{+0.098}_{-0.097}$ and $n = 0.70^{+1.54}_{-1.54}$. For the EoS of IDM, the best-fit value is $w_{\text{IDM}} = -1.23^{+0.51}_{-0.51}$. These results are consistent with the previous results of Basilakos & Plionis (2009) by using fewer observational $H(z)$ data ($n \approx -0.30$ and $w_{\text{IDM}} \approx -0.90$, which favors the effective quintessence model with a constant EoS for which $w > -1$). In Fig. 5, we show the constraint results from SNe Ia. By minimizing the corresponding χ^2 , we find that the best-fit model values

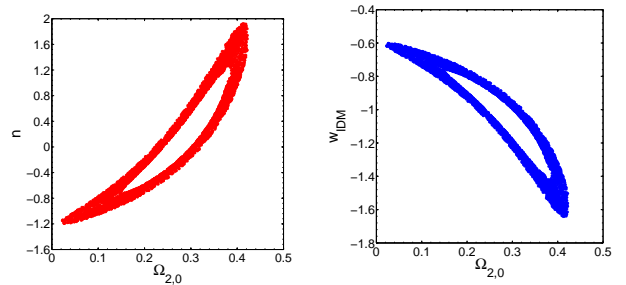


Fig. 5. The likelihood contours at the 68.3% and 95.4% confidence levels in the $\Omega_{2,0} - n$ and $\Omega_{2,0} - w_{\text{IDM}}$ planes provided by fitting model 2 to the SNe Ia data.

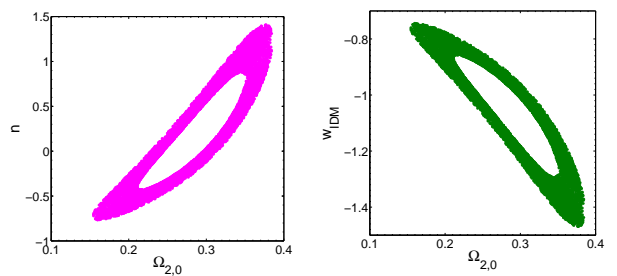


Fig. 6. The likelihood contours at the 68.3% and 95.4% confidence levels in the $\Omega_{2,0} - n$ and $\Omega_{2,0} - w_{\text{IDM}}$ planes provided by fitting model 2 to the $H(z)$ +SNe data.

are $\Omega_{2,0} = 0.288^{+0.108}_{-0.105}$ and $n = 0.17^{+1.10}_{-1.10}$ ($w_{\text{IDM}} = -1.06^{+0.37}_{-0.37}$). For the combined data $H(z)$ + SNe shown in Fig. 6, we find the best-fit values are $\Omega_{2,0} = 0.281^{+0.072}_{-0.071}$ and $n = 0.22^{+0.67}_{-0.66}$ ($w_{\text{IDM}} = -1.07^{+0.24}_{-0.23}$). Obviously, all of the above constraints are consistent with the concordance Λ CDM model and appear to be most consistent with the effective phantom model and a constant EoS for which $w < -1$.

5. Conclusions

We have investigated the interacting dark matter (IDM) scenario mimicking either the Λ CDM model or the w CDM model, which can create the cosmic acceleration without dark energy (Basilakos & Plionis 2009). In our work, the scale of the effective annihilation term κC_1 and therefore the mass of DE particles M_x are constrained with different newly revised observational data including $H(z)$ and Union2 SNe Ia data. When mimicking a Λ cosmology and using three different data combinations of $H(z)$, SNe Ia, and SNe Ia+ $H(z)$, we have found that κC_1 is quite small, which is consistent with the previous results in Basilakos & Plionis (2009), which used fewer observational $H(z)$ data. Meanwhile, for the combined data sets, we obtain a more stringent upper limit to the effective annihilation term with $\log(\kappa C_1 \cdot \text{Gyr}) \approx -3.4$. By relating the range of values of κC_1 to the mass of the DM particle, we have inferred an apparent lower limit of $M_x \approx 10^{-8.6} \text{GeV}$. Furthermore, when mimicking w CDM model and assuming that the particle creation term dominates ($\kappa = 0$), we obtained the effective equation of state of IDM is consistent with the concordance Λ CDM model and appears to be consistent with the effective phantom model with a constant EoS for which $w < -1$.

To sum up, we conclude that the interacting dark matter (IDM) model may provide a practical alternative to Dark Energy in explaining the present cosmic acceleration. The hope of proving this conclusion should be pinned on analyses of future observational data such as high redshift SNe Ia data from SNAP (Albrecht et al. 2006), more precise CMB data from the ESA Planck satellite (Balbi 2007), and complementary data, such as the X-ray gas mass fraction in clusters (Allen et al. 2004; Allen et al. 2008; Ettori et al. 2009), gravitational lensing data (Zhu 1998; Sereno 2002), as well as gamma-ray bursts (GRBs) at high redshift (Schaefer 2007; Liang et al. 2008; Basilakos & Perivolaropoulos 2008; Liang & Zhang 2008; Wang & Liang 2010; Gao et al. 2010; Liang et al. 2011).

Acknowledgements. We thank Yun Chen, Hao Wang, Yan Dai, Chunhua Mao, Fang Huang, Yu Pan, Jing Ming, Kai Liao and Dr. Yi Zhang for discussions. This work was supported by the National Science Foundation of China under the Distinguished Young Scholar Grant 10825313, the Key Project Grants 10533010, and by the Ministry of Science and Technology national basic science Program (Project 973) under grant No. 2007CB815401.

References

- Abraham, R. G., et al. 2004, ApJ, 127, 2455
 Albrecht, A., et al. 2006, Report of the Dark Energy Task Force, arXiv:0609591
 Allen, S. W., et al. 2004, MNRAS, 353, 457
 Allen, S. W., et al. 2008, MNRAS, 383, 879
 Amanullah, R., et al. [Supernova Cosmology Project Collaboration], 2010, ApJ, 716, 712
 Astier, P., et al. 2006, A&A, 447, 31
 Balakin, A. B., Pavon, D., Schwarz, D. J., & Zimdahl, W. 2003, N. J. Phys., 5, 85
 Balbi, A. 2007, New A. R., 51, 281
 Basilakos, S., & Perivolaropoulos, L. 2008, MNRAS, 391, 411
 Basilakos, S., & Plionis, M. 2009, A&A, 507, 47
 Basilakos, S., & Lima, J. A. S. 2010, PRD, 82, 023504
 Bengochea, G. R., & Ferraro, R. 2009, PRD, 79, 124019
 Bento, M. C., et al. 2002, PRD, 66, 043507
 Cao, S., & Liang, N. 2010, arXiv:1012.487
 Caldwell, R., Dave, R., & Steinhardt, P. J. 1998, PRL, 80, 1582
 Caldwell, R. 2002, PLB, 545, 23
 Capozziello, S., & Fang, L. Z. 2002, International Journal of Modern Physics D, 11, 483
 Carroll S. M., Duvvuri V., Trodden M., & Turner M. S. 2004, PRD, 70, 043528
 Chen, Y., Zhu, Z.-H., Alcaniz, J. S., & Gong, Y. G. 2010, ApJ, 711, 439
 Chen, G., Gott, J. R., III, & Ratra, B. 2003, Publ. Astron. Soc. Pac., 115, 1269
 Cirelli, M., Iocco, F., & Panci, P. 2009, JCAP, 10, 9
 Cohen, A., Kaplan, D., & Nelson, A. 1999, PRL, 82, 4971
 Davis, T. M., et al. 2007, ApJ, 666, 716
 Dvali, G., Gabadadze, G., & Porrati, M. 2000, PLB, 485, 208
 Di Pietro, E., & Claeskens, J. F. 2003, MNRAS, 341, 1299
 Ettori, S., et al. 2009, AAP, 501, 61
 Farrar, G. R., & Peebles, P. J. E. 2004, ApJ, 604, 1
 Feng, B., Wang, X., & Zhang, X. 2005, PLB, 607, 35
 Freedman, W. L., et al. 2001, ApJ, 553, 47
 Freese, K., & Lewis, M. 2002, PLB, 540, 1
 Gao, H., Liang, N., & Zhu, Z.-H. 2010, arXiv:1003.5755
 Gaztañaga, E., Cabré, A., & Hui, L. 2009, MNRAS, 399, 1663
 Gong, Y. G., Cai, R. G., Chen, Y., & Zhu, Z.-H. 2010, JCAP, 01, 019
 Gott, J. R., III, Vogeley, M. S., Podariu, S., & Ratra, B. 2001, ApJ, 549, 1
 Gubser, S. S., & Peebles, P. J. E. 2004, PRD, 70, 123510
 Guo, Z.-K., Piao, Y.-S., Zhang, X., & Zhang, Y. Z. 2005, PLB, 608, 177
 Hicken, M., et al. 2009, ApJ, 700, 1097
 Jassal, H. K., Bagla, J. S., & Padmanabhan, T. 2010, MNRAS, 405, 2639
 Jimenez, R., Verde, L., Treu, T., & Stern, D. 2003, ApJ, 593, 622
 Kamenshchik, A., Moschella, U., & Pasquier, V. 2001, PLB, 511, 265
 Kolb, E. W., & Turner, M. S. 1990, The Early Universe, Addison-Wesley Publishing
 Kowalski, M., et al. 2008, ApJ, 686, 749
 Kurek, A., & Szydlowski, M. 2008, ApJ, 675, 1
 Lazkoz, R., & Majerotto, E. 2007, JCAP, 0707, 015
 Lewis, A., & Bridle, S. 2002, PRD, 66, 103511
 Li, M. 2004, PLB, 603, 1
 Liang, N., Xiao, W. K., Liu, Y., & Zhang, S. N. 2008, ApJ, 685, 354
 Liang, N., & Zhang, S. N. 2008, AIP Conf. Proc., 1065, 367
 Liang, N., Gao, C. J., & Zhang, S. N., Chin. Phys. Lett., 2009, 26, 069501
 Liang, N., Wu, P., & Zhang, S. N. 2010a, PRD, 81, 083518
 Liang, N., Wu, P., & Zhu, Z.-H. 2010b, arXiv:1006.1105
 Liang, N., Xu, L., & Zhu, Z.-H. 2011, A&A, 527, A11
 Liang, N., & Zhu, Z.-H. 2010, RAA, in press, arXiv:1010.2681
 Lima, J. A. S., Silva, F. E., & Santos, R. C. 2008, Class and Quantum Gravity, 25, 205006
 Ma, C., & Zhang, T. J. 2011, ApJ, 730, 74
 Nolan, L. A., Dunlop, J. S., Jimenez, R., & Heavens, A. F. 2003, MNRAS, 341, 464
 Nolan, P. L., Tompkins, W. F., Grenier, I. A., & Michelson, P. F. 2003, ApJ, 597, 615
 Peebles, P. J. E., & Ratra, B. 1988a, ApJL, 325, 17
 Peebles, P. J. E., & Ratra, B. 1988b, PRD, 37, 3406
 Perlmutter, S., et al. 1999, ApJ, 517, 565
 Ratra, B., & Peebles, P. J. E. 1988, PRD, 37, 3406
 Riess, A. G., et al. 1998, AJ, 116, 1009
 Riess, A. G., et al. [Supernova Search Team Collaboration], 2004, ApJ, 607, 665
 Riess, A. G., et al. 2007, ApJ, 659, 98
 Riess, A. G., et al. 2009, ApJS, 183, 109
 Sahani, T. D., et al. 2000, PRL, 85, 1162
 Samushia, L., & Ratra, B. 2006, ApJ, 650, L5
 Schaefer, B. E. 2007, ApJ, 660, 16
 Sen, A. A., & Scherrer, R. J. 2008, PLB, 659, 457
 Sereno, M. 2002, A&A, 393, 757
 Simon, J., Verde, L., & Jimenez, R. 2005, PRD, 71, 123001
 Stern, D., et al. 2010, JCAP, 02, 008
 Tammann, G. A., Sandage, A., & Reindl, B. 2008, A&A Rev, 15, 289
 Treu, T., et al. 2001, MNRAS, 326, 221
 Treu, T., et al. 2002, ApJL, 564, L13
 Wan, H. Y., Yi, Z. L., Zhang, T. J., & Zhou, J. 2007, PLB, 651, 352
 Wang, S., Li, X. D., & Li, M. 2010, arXiv:1009.5837
 Wang, T. S. & Liang, N. 2010, ScChG, 53, 1720
 Wei, H., & Zhang, S. N. 2007, PLB, 644, 7
 Wei, H. 2010, JCAP, 08, 020 [arXiv:1004.4951]
 Wilson, K. M., Chen, G., & Ratra, B. 2006, MPLA, 21, 2197
 Wood-Vasey, W. M., et al. 2007, ApJ, 666, 694
 Wu, P. X., & Yu, H. W. 2007a, PLB, 644, 16
 Wu, P. X., & Yu, H. W. 2007b, JCAP, 0703, 015
 Wu, P. X., & Yu, H. W. 2010, PLB, 693, 415
 Xu, L. X., Zhang, C. W., Chang, B. R., & Liu, H. Y. 2008, MPLA, 23, 1939
 Xu, L. X. & Wang, Y. T. 2010a, PRD, 82, 043503
 Xu, L. X. & Wang, Y. T. 2010b, JCAP, 11, 014
 Xu, L. X. & Wang, Y. T. 2010c, arXiv:1009.0963
 Yi, Z. L., & Zhang, T. J. 2007, MPLA, 22, 41
 Zhai, Z. X., Wan, H. Y., & Zhang, T. J. 2010, PLB, 689, 8
 Zhang, T. J., & Ma, C. 2010, arXiv:1010.1307
 Zhang, H. S., & Zhu, Z.-H. 2008, JCAP, 0803, 007
 Zimdahl, W., Schwarz, D. J., Balakin, A. B., & Pavon, D. 2001, PRD, 64, 3501
 Zhu, Z.-H. 1998, A&A, 338, 777
 Zhu, Z.-H., & Fujimoto, M.-K. 2002, ApJ, 581, 1
 Zhu, Z.-H., & Alcaniz, J. S. 2005, ApJ, 620, 7